POSTBUCKLING FAILURE OF COMPOSITE COMPRESSION PANELS

K A Stevens, R Ricci and G A O Davies
Imperial College of Science, Technology and Medicine

Abstract

The initial failure mechanism of a stiffened CFC compression panel has been identified experimentally and the relevant stress resultant measured. When a narrow strip cut from a similar panel is loaded in a special rig to reproduce the deformation seen in the complete panel it is found that the same type of failure occurs and that the magnitude of the stress resultant is similar to that in the complete panel. In conjunction with a nonlinear FE calculation this suggests a method of determining a postbuckling failure load without doing a full scale test.

1. Introduction

Experimental test programmes e.g. Refs 1,2,3,5 and 6, have demonstrated that composite compression panels may have a degree of postbuckling strength, depending upon the particular configuration of the panel. A failure load of twice the buckling load is not exceptional, especially in lightly loaded parts of a structure where the skins will be thin. However, unlike the well-understood behaviour of metal panels, this reserve of strength has not been effectively utilised in the structural design of current composite components in aircraft because of the difficulty in predicting with confidence the failure load.

Researchers who report tests to failure of buckled CFC panels e.g. Refs 1, 2, 3, 5 and 9 often refer to the explosive and destructive nature of the collapse. The damage is usually so comprehensive that evidence which might reveal the initial failure mechanism is destroyed. However, it is invariably the case that collapse following local buckling of the panel is associated with separation of the stiffeners from the skin, involving through thickness or interply stresses. The notorious weakness of laminated composites to these stresses is exacerbated by the complex three-dimensional stress field which exists at the source of failure. It will also be the case that a number of possible failure mechanisms may be feasible at different locations in the panel[9].

To be able to predict the behaviour in the postbuckled state, and the onset and propagation of delamination, it is necessary to perform a nonlinear analysis. The first step in such an analysis is usually a global finite element calculation. This will require a model with a large number of elements in order to represent adequately the details of the stiffener geometry which may be quite complex. For example stiffener flanges are likely to be tapered and the offset from the skin must be reproduced. The computer run will be expensive but will not deliver, a priori, a panel failure load because the details which will influence failure, such as ply curvature, the presence of an adhesive layer, the nature of any ply filler used in forming the stiffener and the way in which plies are dropped off in a tapered flange will not be represented in the global model. A more refined local model will be necessary to predict stiffener debonding, probably needing 2 or 3-D brick idealisation to capture the details of the internal strain fields. But it is still open to question whether, having the stress resultants in the buckled panel from a global analysis, a calculation of the failure load can be performed with the current state of the art of FE modelling and fracture or damage mechanics.

A possible resolution of this difficulty has been proposed in references 6, 7 and 8. These workers suggest that a strength of materials approach is adopted in conjunction with some simple 2-D component tests. For example in Ref 8 McConnell compares the stress resultants calculated in a global FE model at the failure load in the full panel test with the stress resultants measured in a simple pull-off test. The agreement was reported to be

"encouraging". In Ref 6 Hachenberg and Kossira used a transverse strip cut from their blade stiffened test panel. The strip was loaded in four point bending to determine the bending strain at which the flange peeled from the skin starting from the free edge of the flange. They observed that this test, although appropriate for their shear loaded panel might not be correct for a stiffener which carries an axial load. However the work reported in this paper suggests that this may be unduly pessimistic. What is undoubtedly true is the attraction of using a 2-D component strip as a calibrator for the global F.E. prediction, particularly if the strip mimics the failure correctly, without applying the panel compressive load.

Probably the most advanced computer code for the design of efficient postbuckled panels is the development presented in Ref 4. Here Bushnell has provided a link between his PANDA 2, which designs optimum panels, and STAGS which evaluates the design with a full nonlinear analysis. Part of the data input to PANDA 2 is a peel force which is evaluated from a test on a specially made, T-shaped, test piece[3]. This peel force is used in PANDA 2 to determine whether stringer POPOFF is a danger. There is a shortage of evidence on how well the POPOFF calculation is representative of what happens in a panel test to failure. It does seem unlikely that the peel specimen will reproduce failure initiation faithfully, but subsequent crack propagation may be adequately represented.

The work which is presented in this paper is part of a Brite Euram funded investigation into the post-buckling of CFC structures which was carried out in the Aeronautics Department at Imperial College. The subject of the investigation is the postbuckling failure of the I stiffened panel shown in Figure 1. The various possible mechanisms which might lead to disbonding of the stiffener flange were discussed in Ref 9 and the stress resultants were determined in a global FE model at the onset of failure. In this paper component tests are proposed which relate to the failures which have been traced to disbonding of the stiffener at a position opposite the buckle crests. Stress resultants measured in the component tests at failure are then compared with those from the full scale panel.

2. The Test Panels

The test panels, which are manufactured in T300 914C unidirectional prepreg, have four I stiffeners as shown in Figure 1. The stiffeners are either co-cured or bonded to the skin with a layer of B.S.L.322 film adhesive in each case.

The panels were loaded in axial compression under displacement control in a special purpose 250 tonne panel test machine which was designed to have the high stiffness necessary for postbuckling investigations. The unloaded edges were unsupported.

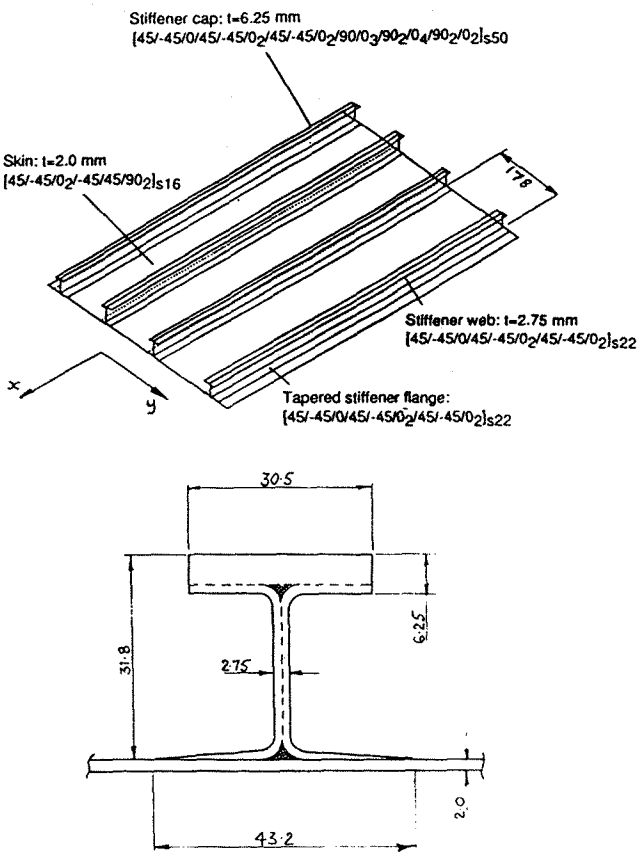

Fig. 1 I stiffened panel 865mm x 610mm and stiffener detail.

The proportions of the panels are such, thin skins and robust stiffeners, that considerable postbuckling strength would be expected, provided the stiffeners are adequately attached to the skin. This indeed proved to be the case.

3. Panel Buckling

Although the computed buckling loads in the local buckling mode are close to each other for 5, 6 or 7 half waves along the panel, the experimental panels in all cases buckled initially with 6 half waves[9]. In the buckled panel the stiffener caps remain essentially straight and the cross section deflects as shown in Figure 2. As the load is increased further the mode shapes remain essentially unchanged except for a tendency, which was shown by all panels, to change to 7 half waves along the length. The change from 6 to 7 half waves would occur suddenly and was accompanied by an audible 'pop'. On unloading the panel the reverse process would occur, without any apparent damage to the panel. This phenomenon of mode switching in the test panels and the implications for the nonlinear computation is discussed in Ref 4.

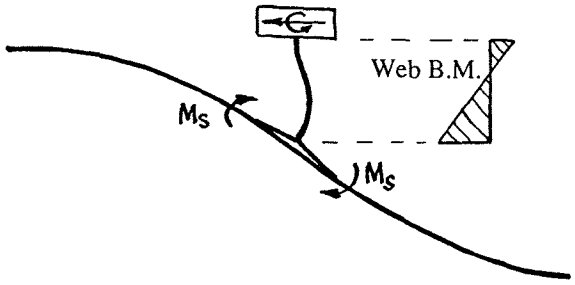

Fig.2 Deformation at an antinode.

4. Test Observations of Panel Failure

4.1 Locations for stiffener debonding

Because of the periodic nature of the deformation it is possible to identify potential failure mechanisms[9]:

(a) At nodal lines the twisting moment in the skin is a maximum so that shear stresses develop between the flange and the skin which will have peak values at the free edge of the flange. Disbonding of the flange will occur if the shear stress reaches a critical value. Tapering of the stiffener flanges is clearly beneficial here.

(b) At anti-nodal lines, where the buckle crests give rise to maximum distortion of the cross section there are two possibilities for flange disbonding.

(i) From Figure 2 we see that the moments in the skin on the right-hand side, Ms, are such as to peel the skin from the flange. Again tapering of the flange will ameliorate this effect by reducing the magnitude of the discontinuity in flexural stiffness. On the left-hand side this moment is such as to hold the flange and skin together, i.e. stabilising.

(ii) The other failure mechanism to be considered at the buckle anti-nodal lines is a consequence of the bending moment in the stiffener web. The thin skin which buckles first interacts with the stiffener tending to twist it in a clockwise direction in Figure 2. The torsional rigidity of the stiffener is almost entirely due to the torsion bending stiffness of the stiffener cap so that the bending moment distribution in the web is as shown, reaching a maximum at the web base. It can be seen that this moment has a tendency to peel away the right-hand flange. The threshold at which this peeling starts depends very much on the highly complex stress field inside the triangle contained between the stiffener flanges and the plate skin to which they are bonded. It is this effect which PANDA 2 calculates from the T peel test data.

4.2 Location and type of initial failure in test panel.

The unsupported edges of the panel consist of a narrow width of skin together with the flange. The relatively high buckling stress of this narrow region has a stabilising effect so that the panel around the two central stiffeners is further into the postbuckling state at any particular load level. Also, because there is some bowing overall, the skin away from the panel ends is more heavily buckled. Thus we might anticipate that failure in one of the modes

described in 4.1 is more likely to occur in the centre regions of the panel.

The initial failure mechanism which characterises the panels tested was that described in b(ii) above. Figure 3 shows a sketch of a buckled panel in which three failures have been detected using ultrasonics. Each failure was accompanied by an audible crack and consists of a crack which ran from the base of the stiffener web outwards under the flange. A typical failure is shown diagramatically in Figure 4. The crack is seen to travel in the first plies of the skin for this co-cured specimen and is always under the flange on the tension side in relation to the web bending moment.

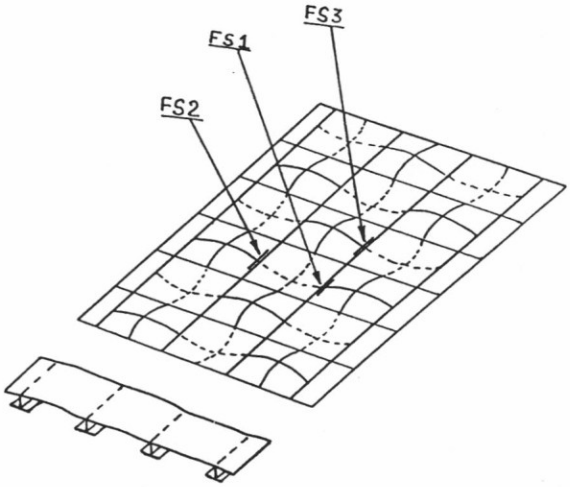

Fig.3 Buckling mode and failure sites.
(Viewed through skin,)

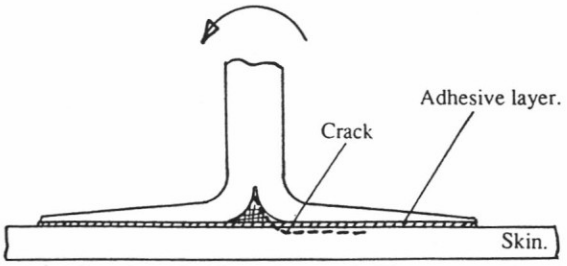

Fig. 4 Failure in a cocured panel.

These cracks extend along the panel for a distance equal to about one half of the buckling half wavelength. With further loading there is no propagation along the length of the panel, but the crack can be made to travel to the free edge of the flange, which will open up over a length of 20 mm [9].

The bending moments in the web have been measured during the tests from strain gauges on both web surfaces and we observed a sudden drop in the web moment when failure was initiated[9]. As the crack propagated out under the flange the moment was further reduced.

4.3 Panel collapse and failure loads

The panels tested buckled at a load of about 11 tonnes and collapsed at a load greater than four times the buckling load, see Table 1. The crack initiation occurred at a load which was close to the final failure load. When a panel with a number of failure sites, as in Figure 3, was taken slowly up to the collapse load, failure was so sudden that the nature of the process from local failure to total collapse was not discernible. The collapsed panel is shown in Figure 5.

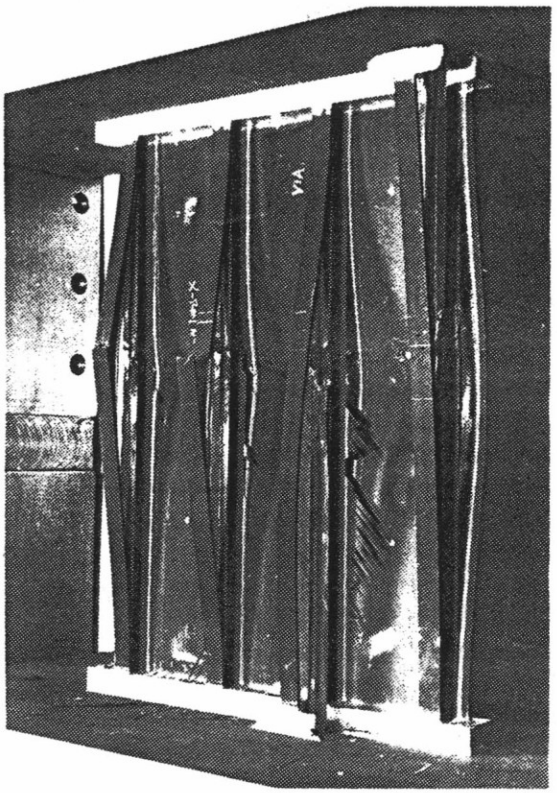

Fig.5 I stiffened panel.
Buckling at 11 tonnes.
Failure at 48 tonnes.

5. Component Tests

Two component tests have been investigated for assessment of the level of stress resultants to produce disbonding of the stiffener flange at the buckle anti-node lines.

5.1 Flange disbonding due to skin bending

In 4.1, b(i) a mode in which the free edge of the stiffener flange disbonded from the skin due to the discontinuity in bending stiffness was identified. Following Ref 6 four point bending tests were done on strips cut from an undamaged panel. The bending moment at which disbonding occurred for four co-cured specimens was very consistent. But a mean bending moment/unit length of 225 N was seen to be much higher than any value of bending moment predicted by the FE analysis at panel failure loading. Hence the absence of any disbonding of the stiffener flanges at their free edges is not unexpected.

5.2 Flange disbonding due to web bending

To estimate the web bending moment associated with disbonding of the stiffener flange a transverse strip from the panel (40 mm wide) was loaded in a special rig. The intention of the rig is to deform the strip in a similar fashion to what happens in the postbuckled panel and to produce a bending moment variation in the web which is representative of the panel test, i.e. with a maximum web bending moment at the web base.

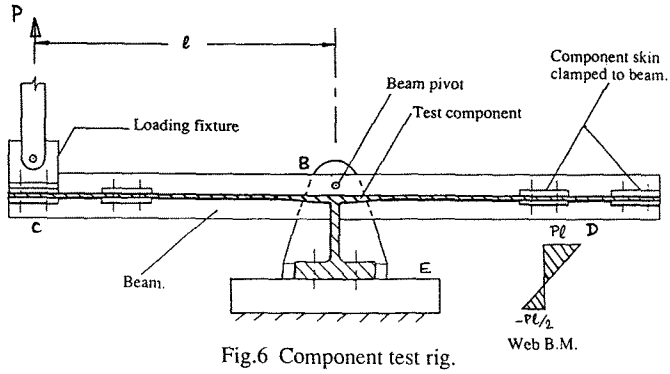

Fig.6 Component test rig.

Figure 6 illustrates the principle. A rigid beam is pivoted about a fixed axis at B by a displacement applied at C. The test piece is bolted through the stiffener cap to a fixed base at E while the skin is clamped to the beam at C and D. The bending moment distribution in the web in terms of the force applied at C is shown in Figure 6.

The limitations of this test as a true representation of the panel arises from its 2-D nature and of course the omission of the axial loading. Not enough results are yet available fully to assess its merit but there is a striking similarity between the micrographs from the panel and the component tests (see Figure 7). Although from Table 1 the component test seems to overestimate the web moment at which cracking occurs, the component test is much more likely than the full scale test to provide information about the nature of the damage mechanism before the unstable crack occurs. In the case of the bonded components acoustic emission signals have indicated that some damage mechanism is active at a mean moment of 275 N, significantly prior to the 'crack' at 365 N.

6. Conclusions

The initial failure mechanism in a particular compression panel design has been identified and an estimate of the stress resultant to produce failure obtained from a 2-D component test.

Not withstanding that the component test does not represent the 3-D character of the loading in a postbuckled panel it does include, by definition, all the features of the manufacturing process.

Although the initial audible cracking suggests unstable propagation, eventually, probably because of the periodic variation of the stress resultants, the damage seems to propagate in a stable fashion.

Further work is in hand to examine theoretically the stress distribution and the fracture characteristics of 2-D models with the objective of being able to predict a stress resultant for failure, without a component test.

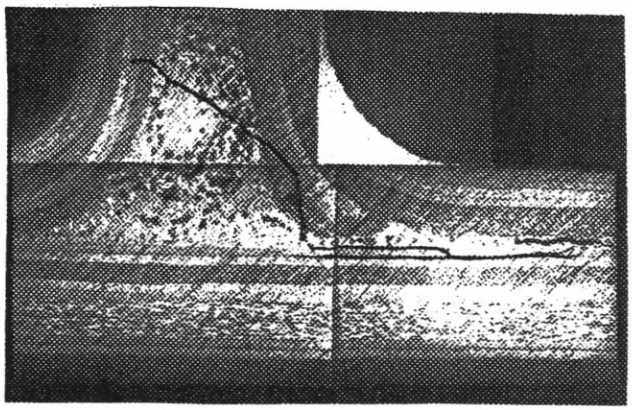

cocured panel

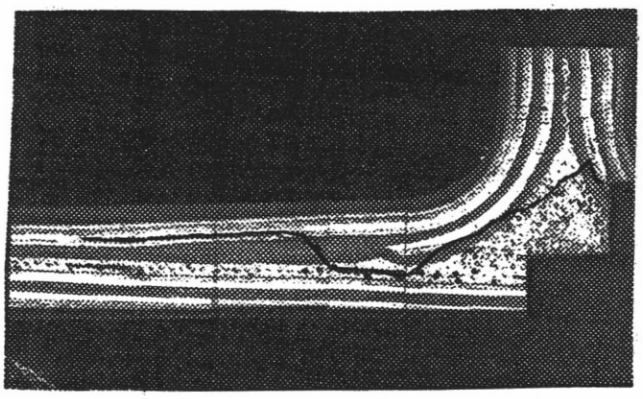

bonded panel

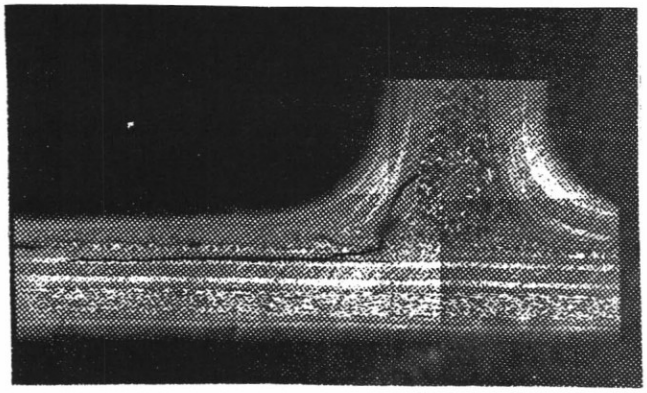

cocured component

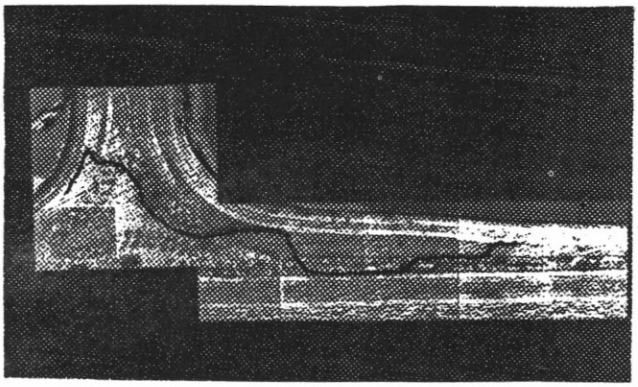

bonded component

Fig.7 Micrographs of failure

	Panel Loads (tonne)			Web BM(N)	
	Buckling	"Crack"	Collapse	"Crack"	Collapse
Bonded Panel	11.75	48.0	46.3	350	352
Bonded Component				365	
Co-cured Panel	11.25	40.7	45.0	315	363
Co-cured Component				342	

Table 1 Panel loads and web bending moments.

7. Acknowledgements

The authors would like to acknowledge the support of the EEC Brite Euram Directive and the co-operation of their colleagues in this joint venture; British Aerospace the project leaders and panel manufacturers, SAAB, Dassault and CASA.

8. References

1. Starnes J H, Knight N F and Rouse M. *Postbuckling behaviour of selected flat stiffened graphite-epoxy panels loaded in compression.* Proc.AIAA/ASME/ ASCE /AHS 23rd Structures, Structural Dynamics and Materials Conf. 1985, Orlando, Florida.

2. Knight N F and Starnes J H. *Postbuckling behaviour of selected curved stiffened graphite-epoxy panels loaded in axial compression.* Proc.AIAA/ASME/ASCE/AHS 26th Structures, Structural Dynamics and Materials Conf. 1985, Orlando, Florida.

3. Bushnell D, Holmes A M C, Flaggs D L and McCormick P J. *Optimum design, fabrication and test of graphite-epoxy, curved, stiffened, locally buckled panels loaded in axial compression.* Buckling of Structures, Ed. I Elishakoff et al. Elsevier Scie. Pub. B.V., Amsterdam, 1988.

4. Bushnell D and Bushnell W D. *Minimum-weight design of a stiffened panel via PANDA 2 and evaluation of the optimised panel via STAGS.* Computers and Structures, Vol 50, No 4, pp 569-602, 1994.

5. Romeo G. *Experimental investigation on advanced composite-stiffened structures under uniaxial compression and bending.* Proc. AIAA/ASME /ASCE/AHS 26th Structures, Structural Dynamics and Materials Conf. 1985, Orlando, Florida.

6. Hachenberg D and Kossira H. *Theoretical and experimental investigation of stringer peeling effects at stiffened shear loaded composite panels in the postbuckling range.* ICAS 1990 pp511-521.

7. Paul P C, Saff C R, Sanger K B, Mapler M A, Kan H P and Kentz E F. *Out of plane analysis for composite structures.* 8th DOD/NASA/FAA Conf on Fibrous Composites in Struct. Design, Norfolk, Virginia, November 1989.

8. McConnell P. *The role of analysis in the design and qualification of composite aircraft structures.* AGARD 74th Struct and Mat Meeting.

9. Stevens K A, Ricci R and Davies G A O. *Buckling and Postbuckling of Composite Structures.* A paper submitted to the journal Composites, 1994.